

Dynamic Properties of a Damper of Torsional Vibrations with Magnetic Impact Pairs

A. M. Guskov^{a,b} and Yu. M. Zamuragin^{b,*}

^a Mechanical Engineering Research Institute of the Russian Academy of Sciences, Moscow, Russia

^b Bauman Moscow State Technical University, Moscow, Russia

*e-mail: yury.zamuragin@yandex.ru

Received August 25, 2020; revised November 21, 2020; accepted December 18, 2020

Abstract—We study the damping efficiency of torsional vibrations of a body using a dynamic vibration damper containing a system of successive impactor pairs with magnets as colliding elements. Dimensionless essentially nonlinear differential equations of motion of the protected body and magnetic elements are obtained. The influence of the designed parameter selection of the vibration damper on the vibrations of the carrying body is considered. The features of damper tuning in a wide vibration damping band mode are described. The optimal variant of damper tuning with the most effective damping of body vibrations is established.

Keywords: dynamic vibration damper, magnetic element, vibration protection, nonlinear dynamics, impact

DOI: 10.3103/S1052618821020072

The creation of high-performance machines and high-speed vehicles, boosted in terms of power, loads, and other indicators of performance, inevitably leads to an increase in the intensity and expansion of the spectrum of vibration effects exerted both on the machine itself and on the environment. To suppress the harmful effects of vibration, various methods and means are used. One of the effective ways to reduce vibration levels is to attach dynamic vibration dampers to a vibrating object [1]. Dynamic dampers are differentiated by the number of degrees of freedom, by the physical principle of the implementation of potential and nonpotential forces, and by the design and other features.

Among the existing variety of principles and design dynamic vibration dampers, vibroimpact action dampers hold a special place [1, 2] providing effective reduction of oscillations in a wide range of excitation frequencies. An essential feature of the structure of any vibroimpact system is the presence of at least one shock pair, which is a combination of two links moving with collisions. In engineering calculations, to take into account the shock interactions of two rigid bodies, the concept of the recovery coefficient upon impact is usually used [2, 3]. It is believed that the value of the recovery coefficient reflects the physical properties of the colliding bodies and does not depend on the impact velocity.

A lot of works by domestic and foreign authors are devoted to consideration of shock vibration dampers. Many of them consider systems with one degree of freedom under different types of external impact [4–10]. Papers [11–17] are also devoted to the use of vibration dampers with several degrees of freedom.

In this article we analyze the efficiency of using a dynamic damper with magnetic shock pairs to reduce the level of torsional vibrations. Earlier, in [18–20], a shock damper of longitudinal vibrations was treated, in which the role of inertial elements is played by permanent magnetic elements and the role of elastic forces is played by magnetic forces. A diagram of this dynamic vibration damper with vibroimpact pairs of magnetic elements is shown in Fig. 1. There are $(n + 2)$ permanent magnets installed in the damper housing so that their like poles are oriented towards each other. The edge magnets, designated by the numbers “0” and “ $n + 1$,” are rigidly fixed on the damper housing.

When exposed to vibration $f(t)$ transmitted to the damper housing, displacement X_i ($i = \overline{1, n}$) of magnets occurs relative to the left edge of the housing. This, in turn, leads to the appearance of repulsive forces F_i , which depend on the distance $b_i(t) = X_i(t) - X_{i-1}(t)$ between neighboring elements (in the position of static equilibrium $b_i(0) = A$). At insignificant amplitudes of external periodic influences, the magnets will

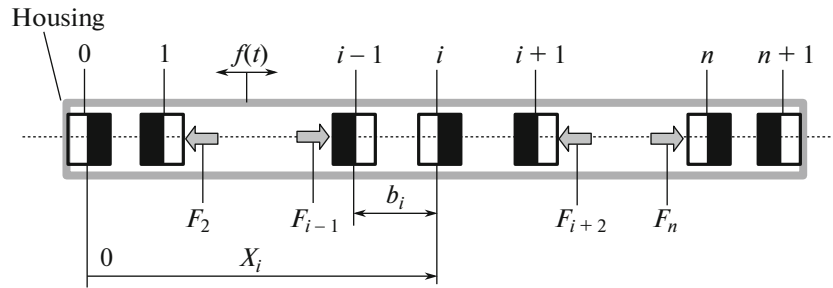


Fig. 1. Vibroimpact dampers with magnetic pairs.

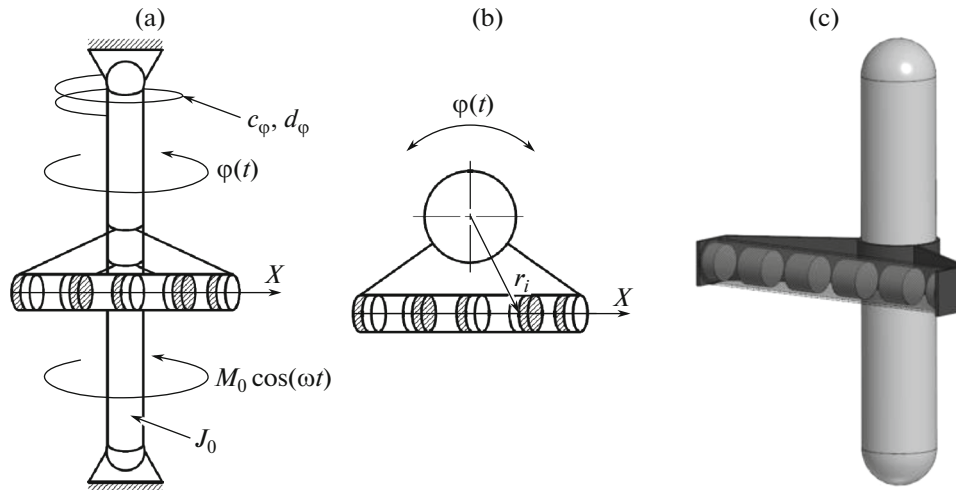


Fig. 2. Installation layout of a dynamic damper on an oscillating shaft: (a) mounting of a damper on the shaft; (b) top view; (c) general view of a body with a damper.

perform impactless movements, while at large amplitudes, vibroimpact modes of movement of magnetic elements are possible.

In [18], the regions of impact and impactless oscillation modes of magnets were obtained on the plane of parameters “the frequency of the external action and the amplitude of the external action.” In [19], the damper efficiency was investigated depending on the distance between the magnetic elements at the initial state of rest, on which the spectrum of the natural frequencies of the device depends. In [20], two types of connection between the damper elements are considered: the analytically obtained magnetic characteristic without correction for experimental data and the case of the absence of magnetic forces between the elements.

Problem statement. The simplest scheme of dynamic damper arrangement on a shaft performing torsional vibrations is shown in Fig. 2. In Fig. 3, as an example, two other possible schemes for symmetrical installation of several dampers in the plane of the shaft cross section are shown.

Without loss of generality, we will consider the scheme of the damper attachment corresponding to Fig. 2. The shaft is assumed to be an absolutely rigid body mounted on bearing supports with the total torsional stiffness c_φ (N) and a damping factor d_φ (kg m²/s). A periodically varying external torque is applied to the shaft:

$$M(t) = M_0 \cos(\omega t), \quad (1)$$

where ω is the torque circular oscillation frequency and t is time. Under the action of the torque, the shaft will perform torsional vibrations with twisting angle $\varphi(t)$. The damper is rigidly attached to the shaft.

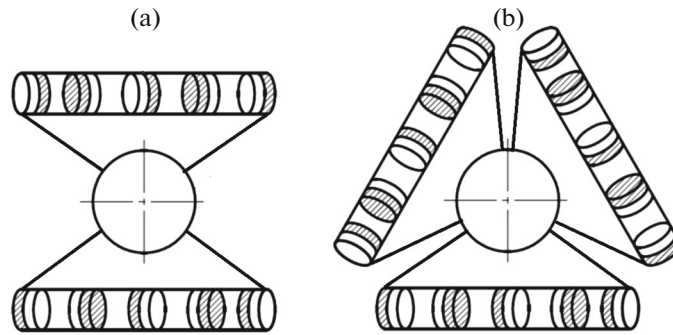


Fig. 3. Attachment scheme of several dampers to a shaft (top view): (a) a body with two dampers and (b) a body with three dampers.

When all the elements of the system vibrate between the magnetic elements, a repulsive force $F_i(z_i)$ arises depending on the dimensionless distance z_i between adjacent magnets (Fig. 1) [19]

$$F_i = F(z_i) = F_0 (z_i - h/2a) / (1 + (z_i - h/2a)^2)^3, \tag{2}$$

where $F_0 = 3\pi B^2 h^2 / 2\mu_0$; $z_i = b_i/a$; h is the height of the cylindrical magnet, m ; B is the residual magnetic induction, T; μ_0 is the magnetic constant $m \text{ kg s}^{-2} \text{ A}^{-2}$; and a is the scaling parameter equal to the radius of the cylindrical magnet, m .

Impact interactions in magnetic pairs, in accordance with the stereomechanical theory of impact, will be taken into account using the recovery factor R [2].

Of particular interest is the study of the conditions for the occurrence of vibroimpact modes. In this article, we also study the efficiency of torsional vibration damping of the shaft, depending on the distance between the magnets at rest (the spectrum of natural frequencies depends on it), the amplitude and frequency of the external torque, and the recovery coefficient upon impact.

Equations of motion. The movements of the system under consideration will be described by the shaft rotation angle ϕ and the movements X_i of each magnet relative to the left edge of the damper. Using the Lagrange equations, we write the differential equations of the system motion in the form

$$\begin{cases} m_i \ddot{X}_i + m_i \ddot{\phi} r_0 - m_i \dot{\phi}^2 X_i + d \dot{X}_i + F_i - F_{i+1} = 0; & i = \overline{1, n}; \\ \left(J_0 + \sum_{i=1}^n m_i r_i^2 \right) \ddot{\phi} + \sum_{i=1}^n m_i \ddot{X}_i r_0 + 2\dot{\phi} \sum_{i=1}^n m_i \dot{X}_i X_i + d_\phi \dot{\phi} + c_\phi \phi = M_0 \cos(\omega t), \end{cases} \tag{3}$$

where m_i is the mass of the i -th magnet, kg ; r_0 is the distance from the axis of the body of rotation to the longitudinal axis of the vibration damper, m ; d is the external damping factor, kg/s ; J_0 is the moment of inertia of the shaft relative to the axis of rotation, kg m^2 ; r_i is the distance from the axis of rotation to the i -th rotating element, m ; F_i and F_{i+1} are the repulsive forces of two neighboring magnets, described by dependences (2), N ; and the “primes” above variables mean derivatives with respect to time, t .

In what follows, the following designations are used for the variables during the transition from the state “before” impact to the state “after” impact: $\{ \}^- \rightarrow \{ \}^+$. The conditions of impact interactions of mobile magnetic pairs and magnetic pairs, in which one of the magnets is rigidly fixed to the housing, are different. In this article, we used two versions of the recovery factors in accordance with [3]: $R = 0.56$ (steel–steel impact) and $R = 0.94$ (glass–glass impact).

The impacts of internal magnetic elements against each other are described by the relations

$$\begin{cases} X_{i-1}^+ = X_{i-1}^-, \\ X_i^+ = X_i^-, \\ \dot{X}_{i-1}^+ = ((m_{i-1} - Rm_i) \dot{X}_{i-1}^- + m_i (1 + R) \dot{X}_i^-) / (m_{i-1} + m_i), \\ \dot{X}_i^+ = (m_{i-1} (1 + R) \dot{X}_{i-1}^- + (m_i - Rm_{i-1}) \dot{X}_i^-) / (m_{i-1} + m_i). \end{cases}$$

Table 1. Variable parameter values

No.	Recovery coefficient, R	External torque amplitude, M_0	External perturbation frequency, ν	Distance between magnets at a state of rest, α
1	Without impact	0.024	$\nu = \nu_0 = 0.059$	0.43
2	0.56	0.135	$\nu = \nu_0 = 0.059$	0.43
3	0.56	5×10^{-4}	$\nu = [0.8\nu_0, 1.2\nu_0]$	$\alpha_1 = 0.43, \alpha_2 = 1.15$
4	0.94	5×10^{-4}	$\nu = [0.8\nu_0, 1.2\nu_0]$	$\alpha_3 = 1.56, \alpha_4 = 1.79$

In contrast to the damper of longitudinal vibrations, in this case, the impact of a movable magnet with a relatively stationary magnet is taken into account with conservation of the angular momentum

$$\begin{cases} X_i^+ = X_i^-, \\ \phi^+ = \phi^-, \\ \dot{X}_i^+ = -R\dot{X}_i^-, \\ \phi^+ = \left[(m_i\dot{X}_i^-(1+R)r_i) / (m_i r_i^2 + J_0) \right] + \phi^-. \end{cases}$$

In order to reduce mathematical model (3) to a dimensionless form, we introduce the linear scale $X_* = a$, m, the time scale $T_* = \sqrt{ma/F_0}$, and dimensionless complexes and variables

$$\begin{aligned} \kappa &= c_\phi T_*^2 / ma^2, \quad \zeta = dT_* / 2m, \quad \zeta_\phi = d_\phi T_* / 2ma^2, \\ \theta_i &= r_i / a, \quad M_0 = M_0 / Fa, \quad \nu = \omega T_*, \quad \tau = t / T_*, \\ \Phi_i &= F_i / F_0, \quad \alpha = A / a, \quad J = J_0 / ma^2, \\ \xi_i &= X / a, \quad \xi_i' = T_* \dot{X}_i / a, \quad \xi_i'' = T_*^2 \ddot{X}_i / a, \\ \phi &= \varphi, \quad \phi' = T_* \dot{\varphi}, \quad \phi'' = T_*^2 \ddot{\varphi}. \end{aligned} \quad (4)$$

Having substituted (4) into (3), we obtain the equation of the system of motion in dimensionless form

$$\begin{cases} \xi_i'' + \theta_0 \phi'' - \phi' \xi_i + 2\zeta \xi_i' + \Phi_i - \Phi_{i+1} = 0; \quad i = \overline{1, n}; \\ \phi'' \left(J + \sum_{i=1}^n \theta_i^2 \right) + \sum_{i=1}^n \xi_i'' \theta_0 + 2\phi' \sum_{i=1}^n \xi_i \xi_i' + \kappa \phi + 2\zeta_\phi \phi' = M_0 \cos(\nu\tau), \end{cases}$$

where the “prime” means the derivative with respect to dimensionless time τ .

In the calculations (except for the amplitude–frequency characteristics), a damper with five impactor pairs (four movable magnets and two fixed on the body) was used, the first frequency of which is equal to the natural frequency of the body. This procedure is described in [19]. Numerical calculations were carried out using the MATLAB software package for the following values of constant system parameters:

$$\begin{aligned} n &= 4, \quad \zeta = 9.56 \times 10^{-5}, \quad \zeta_\phi = 2.65, \quad J = 1.31 \times 10^4, \\ J_* &= 0.19J, \quad \nu_0 = 0.059, \quad \kappa = 53.79, \end{aligned}$$

where n is the number of movable magnets; J_* is the ratio between the damper inertia moment relative to the axis of rotation of the body and the moment of inertia of the body without a damper; and $\nu_0 = \sqrt{\kappa/J}$ is the natural vibration frequency of the protected body.

An assessment of the influence of individual parameters on the calculation results was carried out for the values given in Table 1.

Figure 4 shows the results of numerical simulation for the oscillations of the body-vibroimpact damper system under an external influence, which does not lead to the occurrence of impact modes.

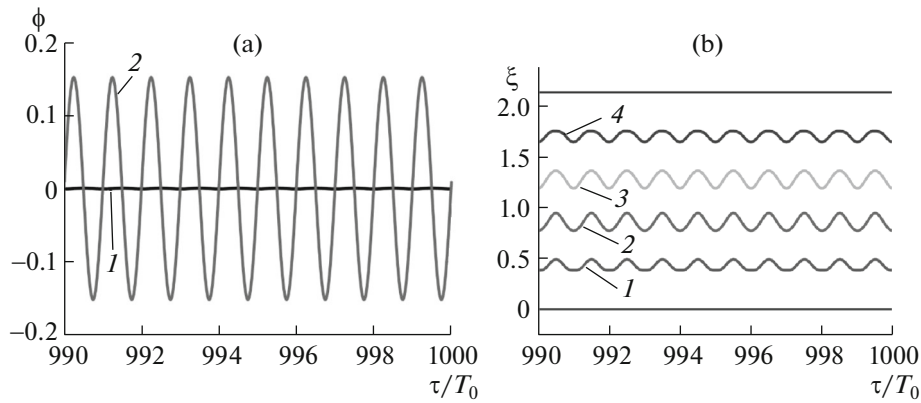


Fig. 4. Graphs of oscillations of (a) a vibration-isolated body and (b) magnetic elements in impactless mode.

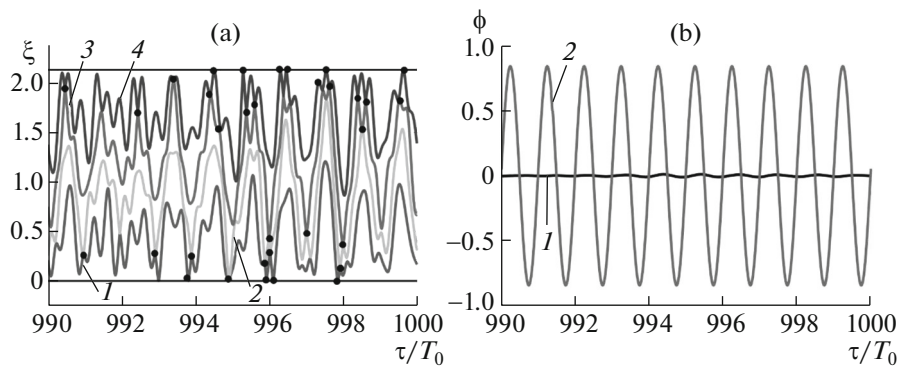


Fig. 5. Graphs of vibrations of magnetic elements (a) during their collisions and (b) a vibration-isolated body.

One can see from Fig. 4 that the system performs periodic oscillations with a period equal to the period of external influence. It is important to note that, in this case, the oscillation amplitude of a body with a vibroimpact damper (Fig. 4a, curve 1) is approximately 250 times less than the amplitude of oscillations of a body without a damper (Fig. 4a, curve 2). The oscillation plots of four movable magnetic elements relative to the damper housing are shown in Fig. 4 by straight lines 1–4.

Figure 5 plots the results of calculation of oscillations of the system with the amplitude of the external action at which the impact modes take place.

Black dots in Fig. 5a indicate the moments of collisions between the elements of the system. With this external influence, the oscillations of magnets are no longer periodic and irregular impact interactions appear. The amplitude of vibrations of a body with vibration damper (Fig. 5b, curve 1) in this case decreases by approximately 74 times as compared to the amplitude of vibrations of a body without a damper (Fig. 5b, curve 2).

Amplitude–frequency responses. To assess the effectiveness of tuning of the oscillation damper depending on the ratio of the natural frequencies of the damper and the body, the ratio of the amplitude–frequency responses of body oscillations with and without a damper (the vibration damping efficiency factor) is used. Figures 6 and 7 show the corresponding plots. Curves 1–4 correspond to the four options for setting the oscillation damper (each natural frequency of the damper is tuned to the natural frequency of oscillation of the body and denoted by the same number with the curve), and line 5 shows the amplitude–frequency response without a damper. Figure 6 shows the results of numerical calculations with the parameters indicated in the third row of Table 1. It is important to note that, even with a relatively small amplitude of external influence, impact modes are observed. This is confirmed by the nonsmoothness of the curves in Fig. 6.

The result demonstrates that the damper is most effective, the first natural frequency of which is tuned to the external action frequency: vibrations of the body with a vibration damper are practically absent

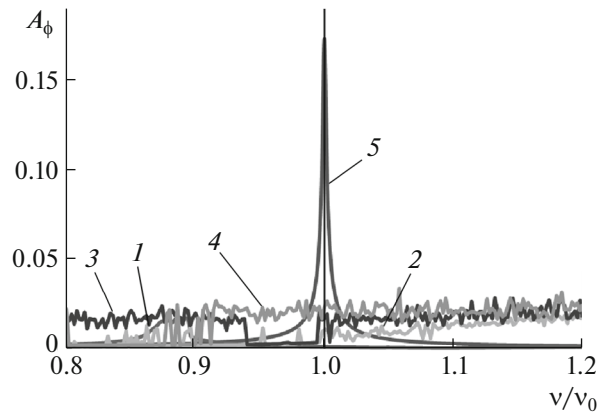


Fig. 6. Amplitude–frequency responses of a body with and without a damper at $R = 0.56$.

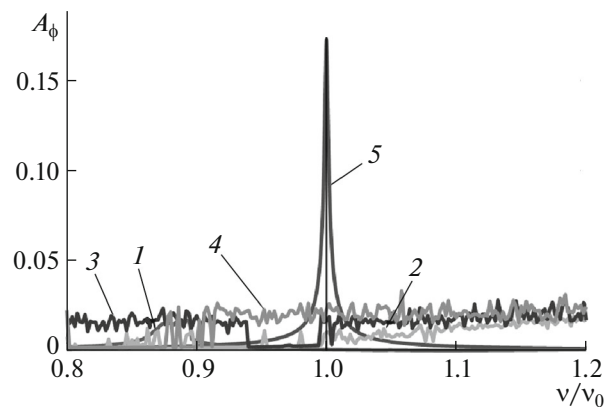


Fig. 7. Same as in Fig. 6 for $R = 0.94$.

throughout the considered frequency range of external influences and the modes of movement are mostly impactless. The rest of the damper adjustment options also effectively reduce the body oscillation amplitudes in the range considered, but the driving modes are mainly impact ones.

Figure 7 plots the calculated amplitude–frequency response with the recovery factor $R = 0.94$ upon impact (Table 1, line 4).

In this case, the maximum vibration damping efficiency is also observed when using a damper with the first natural frequency equal to the frequency of the external influence. One can see that the rest of the dampers, with the use of which the impact oscillation modes arise, lead to larger values of the oscillation amplitudes of the body in comparison with the same dampers having a lower recovery coefficient upon impact (Fig. 6).

CONCLUSIONS

The use of the proposed device as a dynamic oscillation damper effectively reduces the vibration amplitude of a damped body. An especially effective damper is that in which the first natural frequency is equal to the frequency of the external action. When tuning other frequencies of the damper to the frequency of the external impact, its efficiency is approximately the same and rather high in all cases considered.

FUNDING

This work was supported by the Russian Foundation for Basic Research, project no. 19-19-000065.

CONFLICT OF INTEREST

The authors declare that they have no conflict of interests.

REFERENCES

1. Chelomei, V.N., *Vibratsii v tekhnike: Zashchita ot vibratsii i udarov: Spravochnik* (Vibration in Technology: Protection against Vibration and Shock: Handbook), Moscow: Mashinostroenie, 1981, vol. 6.
2. Babitskii, V.I., *Theory of Vibroimpact Systems*, Moscow: Nauka, 1978.
3. Targ, S.M., *Kratkii kurs teoreticheskoi mekhaniki: Ucheb. dlya vtuzov* (A Short Course in Theoretical Mechanics: Handbook), Moscow: Vyssh. Shk., 1986.
4. Vul'fson, I.I., On the problem of dynamic damping of torsional oscillations of a machine drive, *J. Mach. Manuf. Reliab.*, 2009, vol. 38, pp. 13–18.
5. Gus'kov, A.M., Panovko, G.Ya., and Chan Van Bin, Analysis of the dynamics of a pendulum vibration absorber, *J. Mach. Manuf. Reliab.*, 2008, vol. 37, pp. 321–329.
6. Dukart, A.V. and Thanh Binh Pham, Free vibrations of a single-mass system with a single-acting shock absorber, *Vestn. Mosk. Gos. Stroit. Univ.*, 2011, no. 8, p. 164.
7. Dukart, A.V. and Thanh Binh Pham, Stationary oscillations of a system with a shock absorber under the action of periodic pulses of finite duration, *Vestn. Mosk. Gos. Stroit. Univ.*, 2012, no. 4, p. 44.
8. Erokhina, T.V., Sinev, A.V., and Stepanova, L.A., Frequency properties of a dynamic damper with inertial transducer, *J. Mach. Manuf. Reliab.*, 2011, no. 4, p. 37.
9. Chernikov, S.A., Expansion of the suppression band of a vibroprotective system by a feedback dynamic damper, *J. Mach. Manuf. Reliab.*, 2015, no. 5, p. 54.
10. Timofeev, G.A., Lyuminarskiy, I.E., and Lyuminarskiy, S.E., To calculation of shock vibration suppressors of unilateral action, *Herald Bauman Moscow State Tech. Univ., Ser. Mech. Eng.*, 2019, no. 1, p. 90.
11. Makarov, S.B., Pankova, N.V., and Tropkin, S.N., The use of passive multifrequency dynamic vibration dampers (MDVD) in seismic protection problems, *Seism. Stroit., Bezop. Sooruzh.*, 2016, no. 6, p. 42.
12. Makarov, S.B., Pankova, N.V., and Perminov, M.D., Investigation of elastic structures partially filled with liquid as multifrequency dynamic vibration dampers (MDVD), *J. Mach. Manuf. Reliab.*, 2016, no. 2, p. 78.
13. Makarov, S.B., Pankova, N.V., and Perminov, M.D., A model problem on the use of a multifrequency dynamic vibration damper (MDVD) on an object with eigenmodes of various types of vibration, *Probl. Mashinost. Avtom.*, 2017, no. 4, p. 103.
14. Manzhosov, V.K. and Novikov, D.A., *Modelirovanie perekhodnykh protsessov i predel'nykh tsiklov dvizheniya vibroudarnykh sistem s razryvnymi kharakteristikami* (Modeling of Transient Processes and Limiting Cycles of Motion of Vibroimpact Systems with Discontinuous Characteristics), Ulyanovsk: Ulyanovsk. Gos. Tekh. Univ., 2015.
15. Bapat, C.N. and Sankar, S., Multiunit impact damper – re-examined, *J. Sound Vib.*, 1985, vol. 103, no. 4, p. 457.
16. Lu, Z., Masri, S.F., and Lu, X., *Particle Damping Technology Based Structural Control*, Springer, 2020.
17. Ye, H., et al., Experimental study on the damping effect of multi-unit particle dampers applied to bracket structure, *Appl. Sci.*, 2019, vol. 9, no. 14, p. 2912.
18. Zamuragin, Yu.M. and Gus'kov, A.M., Amplitude–frequency characteristic of a vibroimpact system with magnetic elements, *XXX Mezhdunarodnaya Innovatsionnaya konferentsiya molodykh uchenykh i studentov (MIKMUS-2018)* (XXX International Innovative Conference of Young Scientists and Students (MIKMUS-2018)), 2019, p. 304.
19. Zamuragin, Y.M., Gouskov, A.M., and Krupenin, V.L., Damping of oscillations by a vibro-impact system with serial magnetic impact pairs, in *Nonlinear Wave Dynamics of Materials and Structures*, Cham: Springer, 2020, p. 423.
20. Zamuragin, Y.M., Gouskov, A.M., and Krupenin, V.L., Influence of communication between elements in a dynamic damper on a vibrated body behavior, *IOP Conf. Ser.: Mater. Sci. Eng.*, 2020, vol. 747, artic. no. 012064.

Translated by G. Dedkov